

SCIENTIFIC REPORTS



OPEN

Detecting and modelling delayed density-dependence in abundance time series of a small mammal (*Didelphis aurita*)

Received: 12 June 2015
Accepted: 01 December 2015
Published: 11 February 2016

E. Brigatti¹, M. V. Vieira², M. Kajin³, P. J. A. L. Almeida⁴, M. A. de Menezes^{5,6} & R. Cerqueira²

We study the population size time series of a Neotropical small mammal with the intent of detecting and modelling population regulation processes generated by density-dependent factors and their possible delayed effects. The application of analysis tools based on principles of statistical generality are nowadays a common practice for describing these phenomena, but, in general, they are more capable of generating clear diagnosis rather than granting valuable modelling. For this reason, in our approach, we detect the principal temporal structures on the bases of different correlation measures, and from these results we build an ad-hoc minimalist autoregressive model that incorporates the main drivers of the dynamics. Surprisingly our model is capable of reproducing very well the time patterns of the empirical series and, for the first time, clearly outlines the importance of the time of attaining sexual maturity as a central temporal scale for the dynamics of this species. In fact, an important advantage of this analysis scheme is that all the model parameters are directly biologically interpretable and potentially measurable, allowing a consistency check between model outputs and independent measurements.

One of the main objectives in the field of population dynamics is to determine the extent of deterministic vs. stochastic forces in time series of abundance and population parameters. The deterministic share of the observed fluctuations is usually assigned to nonlinear density-dependent processes, which create regulatory and stabilising forces¹. Different theoretical and modelling frameworks have been used through the history of population dynamics, but time series analysis and autoregressive models are a frequent and natural choice, as the population size in the future is related to the population size in the past^{2–4}. A variety of time series analysis methods have been used in population dynamics to diagnose their structure and density dependence⁵, particularly successful in the analysis of empirical data of long lived taxa such as mammals^{6–8}. The approach proposed by Royama⁹ combines diagnostic tools with the use of phenomenological models, and has increased the predictive power and understanding of the dynamics of intensively studied systems^{10–12}. In general, for sufficiently long time series, it is possible to use conventional autoregressive models or to apply other analogous methods which aim to determine a clear differentiation between deterministic and random components^{13,14}. The most common approach^{9,15} uses a linear autoregressive model of order k , which relates the logarithm of the population abundance (y_t) at different time steps:

$$y_t = \beta_0 + \sum_{i=1}^k \beta_i y_{t-i} + \varepsilon_t. \quad (1)$$

¹Instituto de Física, Universidade Federal do Rio de Janeiro, Av. Athos da Silveira Ramos, 149, Cidade Universitária, 21941-972, Rio de Janeiro, RJ, Brasil. ²Laboratório de Vertebrados, Instituto de Biologia, Universidade Federal do Rio de Janeiro. Caixa Postal 68020, 21941-590, Rio de Janeiro, RJ, Brasil. ³Laboratório de Ecologia de Mamíferos, Departamento de Ecologia, Instituto de Biologia Roberto Alcântara Gomes, Universidade do Estado do Rio de Janeiro, Campus Maracanã, 20550-900, Rio de Janeiro, RJ, Brasil. ⁴Coordenação de Matemática Aplicada, Laboratório Nacional de Computação Científica, 25651-075, Petrópolis, RJ, Brasil. ⁵Instituto Nacional de Ciência e Tecnologia de Sistemas Complexos, 22290-180, Rio de Janeiro, RJ, Brasil. ⁶Instituto de Física, Universidade Federal Fluminense, Campus da Praia Vermelha, 24210-340, Niterói, RJ, Brasil. Correspondence and requests for materials should be addressed to E.B. (email: edgardo@if.ufrj.br)

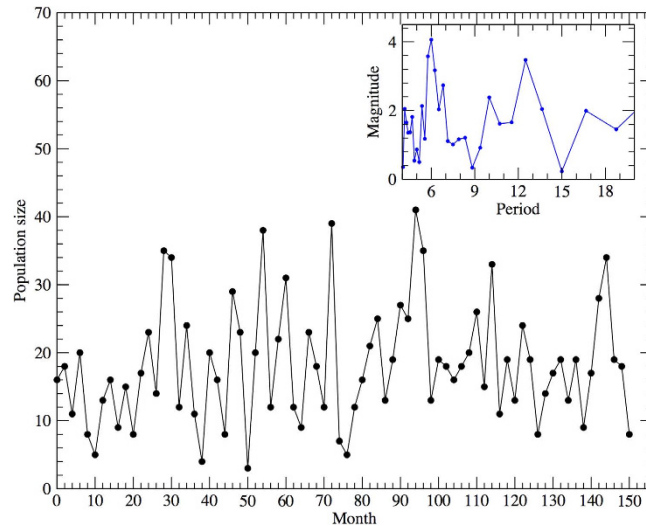


Figure 1. The time series used, comprised of bimonthly estimated local population sizes of a *Didelphis aurita* population in the Brazilian Atlantic forest, State of Rio de Janeiro, from April 1997 to October 2009. In the inset, the magnitude of the Discrete Fourier Transform of the data against the period.

As ε_t represent a random component, this is an ordinary $AR(k)$ model, where the k -value can be determined implementing an AIC-based selection. This approach is equivalent to fitting the population growth rate and it is efficient in determining density dependence. Considering that the correct estimation of the order of the model can be critical, that the real process can be highly nonlinear^{9,16}, and that a direct connection between parameters β_t and demographic estimated quantities is difficult, in general, the most appropriate role of this method is diagnosis rather than modelling¹⁷. Finally, taking into account that the random component included in population size time series can be difficult to characterise¹⁸, and that time series of the necessary length are not so common, it may be reasonable to take the reverse path. Instead of trying to diagnose and project the exact time series behaviour based on a general autoregressive model of a given order, it can be more informative to make inferences about its statistical properties and patterns of variance, and use these results to elaborate a specific and realistic dynamical model. Finally, the parameters of this particular model may be estimated by a standard autoregressive procedure.

Here in we use diagnostic tools to characterise the structure of a 13-year time series of population size estimates of a Neotropical marsupial, the black-eared opossum, *Didelphis aurita* (Wied-Neuwied 1826), and develop a simple model that successfully reproduces its population dynamics. First, we determine periodicity, autocorrelations structures and the nature of potentially density dependent regulation. Second, we use this diagnosis to build a simple model, incorporating the characteristics of the series. Third, we estimate the parameters of such a model. Finally, we compare the observed series with the ones generated by the model as an empirical test of model fit to the data, and of the whole procedure of model development. Models generated by this procedure can be simpler compared to some aspects of previous approaches, and yet still incorporate the main drivers of the dynamics. The simple model developed for *D. aurita* is capable of reproducing the time series dynamic behaviour and all their parameters are biologically interpretable and measurable in term of basic demographic quantities.

Materials and Methods

We analysed a 13-year time series of local population size estimates of black-eared opossums. The data set originated from the long-term small mammal population-monitoring program performed by Laboratório de Vertebrados, Universidade Federal do Rio de Janeiro, within the Parque Nacional da Serra dos Órgãos, state of Rio de Janeiro (22° 28' 28" S, 42° 59' 86" W, details in¹⁹). The local population sizes were estimated using program MARK²⁰. To minimise census error, accurate population size estimates were obtained in a two-step modelling procedure: we first tested for the existence of heterogeneity in capture probabilities, then, having evidence of the existence of the latter, we used the appropriate estimator, namely, the Jackknife estimator to obtain population size estimates. Different models were fitted to the data, where the candidate model set comprised models including temporal variation in all real parameters and all nested models within this global model. The model that was best supported by the data was chosen based on the maximum likelihood principle (using QAICc index, corrected for possible data over-dispersion)²¹.

The time series used in the analyses ($X_{t=1,2,\dots,76}$) represents the estimated bimonthly local population sizes from April 1997 to October 2009 (see Fig. 1). Most studies of mammal populations analyse abundance counts or estimates using annual data^{22–24}, and rarely populations are analysed on a finer time scale, using seasonal²⁵ or monthly abundances²⁶. Annual abundances are more commonly used when the aim is to describe long term behaviours, the organism has a defined and limited reproductive season within the year, or simply because data on a finer time scale are not available. In our case, reproduction of *D. aurita* occurs during a large portion of the year with no single reproductive peak, having two or up to three litters within a year^{19,27,45}. Moreover, population

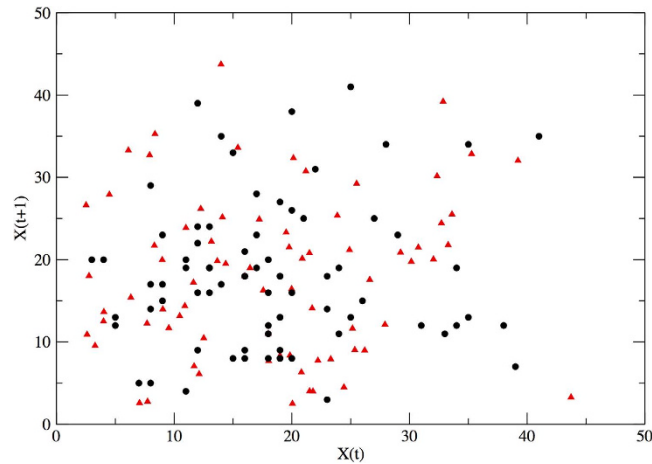


Figure 2. Comparison of the observed $X(t+1)$ versus $X(t)$ (black circles) with the iterates of the best-fit model parametrised as in Table 1 with added noise (red triangles).

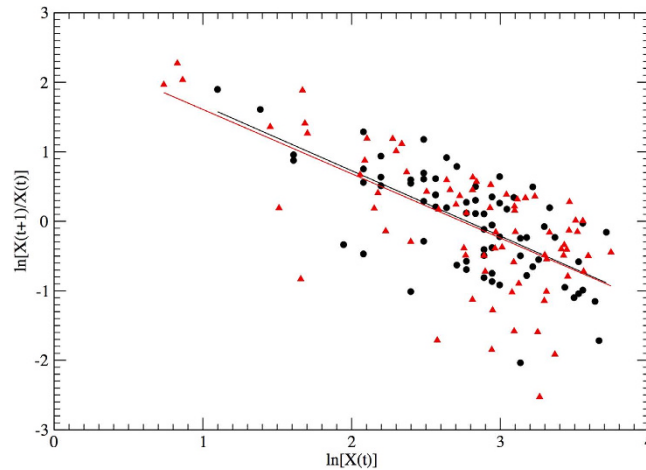


Figure 3. Observed log growth rate versus log abundance (black circles), with iterates of the best-fit model with the parameters of Table 1 and the added noise (red triangles). The black line represents the linear fit for the real data: $\log \frac{X(t+1)}{X(t)} = 2.61 - 0.94 \times \log X(t)$, and the red one for the simulated data: $\log \frac{X(t+1)}{X(t)} = 2.53 - 0.93 \times \log X(t)$.

size fluctuations may not be related exclusively to reproductive events: immigrations to and emigrations from the area may occur²⁸, modifying the local population size on a time scale that is not season or year-related. At the same time, both of these processes may be density dependent. Therefore, the appropriate temporal scale to investigate changes in abundance and regulatory processes must be thinner than a year. This suit of life history traits is common to other populations of neotropical marsupials²⁹, hence seasonal or monthly time scales are likely the most appropriate.

As a first step, we try to identify basic patterns that clearly deviate from pure random behaviour. These basic patterns should be capable of summarising statistical and dynamical behaviours, with attention to the broad essential structures rather than the specific details. We emphasise that our time series is still not long enough to consider particular quantitative numerical outputs of the statistical analyses, but rather we limited our considerations to the qualitative behaviour delineated by our examination.

The standard plot of $X(t+1)$ against $X(t)$ shows a uniform distribution of points suggesting that no threshold-like behaviour or elementary correlations exist in our data (see Fig. 2). The plot of the logarithm of the population growth rate $\left(\log \frac{X(t+1)}{X(t)}\right)$ as a function of the logarithm of the population number ($\log X(t)$) shows that the growth rate clearly declines as population size increases (see Fig. 3). The relationship seems also characterised by a larger variance at high population sizes but it is difficult to characterise this effect because of the small sample sizes at low abundances. This behaviour in the variance can be generated by involved interactions between process errors (biotic and abiotic) and observation errors. Estimation of these different sources of error is not possible, and out the scope of this study.

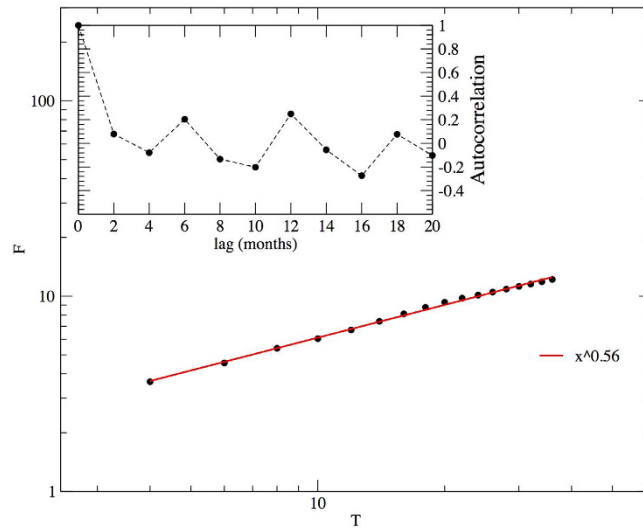


Figure 4. DFA analysis of the abundance time series. The red line represents the fit: $F(T) = 1.7 \times T^{0.56 \pm 0.01}$. In the inset, the autocorrelation function of the same dataset.

We performed a spectral analysis of the data, which does not present any robust or clear periodicity, except for some more prominent modes in correspondence of the 6-month time lag and its multiples (see inset of Fig. 1). We continued our inspection with the study of the autocorrelation function. Its behaviour reveals an interesting periodical structure (inset of Fig. 4), where positive autocorrelations were found for 6-month time lag and its multiples. The strongest negative autocorrelation values appear always four months after the positive peaks.

We explored the long term behaviour of correlations looking at the scaling of the time-series fluctuations at different time lags. Power-law scalings in population fluctuations, which display a clear deviation from pure random behaviours, are well known fact reported in the literature³⁰. The direct inspection of autocorrelations is usually not appropriate because of noise effects and because of possible non-stationarities³¹. In contrast, a robust and general method for the characterisation of the fluctuations behaviour at different scales is the detrended fluctuation analysis (DFA)³¹. It measures the second moment-fluctuation F of the detrended time series for different time windows of size T , obtaining $F = F(T)$. The scaling behaviour is characterised by estimating the exponent α , a generalisation of the Hurst exponent, which is extracted from the relation $F(T) \propto T^\alpha$. A straightforward way for its evaluation is a linear fit of the log-log graph of $F(T)$ as a function of T (Fig. 4). For our time series we obtain $\alpha = 0.56 \pm 0.01$, which is significantly different from the case of uncorrelated, white noise series, characterised by $\alpha = 1/2$. Considering that the exponent is not very far from $1/2$ and that the regression is realised on less than two decades, we are lead to interpret these outcomes just as a detection of positive autocorrelations rather than a claim about the self-similarity of the time series. For this reason we use the DFA method for clearly identifying positive correlations, not for conclusively assessing their power-law scaling^{32,33}.

We can summarise the principal results of this analysis outlining two basic patterns present in our data. First, a clear trend in the growth rate which declines for large population sizes⁶. This effect suggests the presence of some type of density dependent regulation in the population dynamics. Second, the autocorrelation analysis sketch out a positive correlation for lag multiples of six months, followed by a negative one four months later. These results are corroborated by the DFA analysis, where we can outline a deviation from an uncorrelated, white noise time series ($\alpha > 1/2$), which indicates some type of long-memory process that generates correlations between the data³⁴. These outcomes indicate a possible time delay in the density effect on natality and suggest the use of some delayed-recruitment model for the replication of the time series.

Starting from these results we assemble one of the simplest autoregressive models which could account for such basic patterns. In fact, as we study a specific population, it is more appropriate to build in its specific mechanisms and patterns, rather than to bother with claims of statistical generality. We begin from the simplest recurrence relation $x_t = ax_{t-1}$, where x_t denotes the population size at time t . Each period t represents two months, which correspond to the time scale of field data collection. A recruitment term must be added, which can account for the detected structure in the correlation of the time series, and takes into consideration that sexual maturity in this population takes place only 6 months after birth²⁷. For these reasons, we add a second term $G(x_{t-\tau})$ where $x_{t-\tau}$ is the adult breeding population, which is selected with a delay of τ periods. An analogous model has been used for studying baleen whale populations^{35,36}. The final strategy is to make the minimalistic assumption about the form of $G(x_{t-\tau})$ which could describe the outlined density dependent growth rate. A common one is a quadratic polynomial, which leads to the following autoregressive model:

$$x_t = ax_{t-1} + bx_{t-\tau} + cx_{t-\tau}^2 + \varepsilon_t. \quad (2)$$

Here ε_t stands for some stochastic term affecting the population abundance x_t and, as a starting approximation, we model it with a normally distributed noise $N(0, \sigma^2)$. The autoregressive coefficients can be obtained by least-squares estimates: we minimise the squared difference between the modelled time series and the observed

one³⁷. We based our model on the observed value of the population abundance X_t , but the use of the $\log X_t$ generates very similar results.

Finally, we must determine the value of τ . This is attained identifying which is best at predicting the observed data. The accuracy of our prediction is measured using the following quantity³⁸:

$$R^2 = 1 - \frac{\sum_{i=1+\tau}^{76} (X_i - \widehat{X}_i)^2}{\sum_{i=1+\tau}^{76} (X_i - \bar{X})^2} \quad (3)$$

where \widehat{X}_i are the predicted values, X_i are the observed ones and \bar{X} is their mean value. $R^2 = 1$ represents a perfect prediction and accuracy reduces with decreasing in R^2 value. We draw attention to the fact that negative values are a possible output since we are not simply fitting our values with a regression, but we are trying to predict future values with an autoregression³⁸. In particular, negative values indicate that prediction is even worse than using the mean of the series. This quantity can be used for determining the best τ value only because the number of model parameters is fixed, and it does not change with the value of τ , like in the approach presented in equation 1. Finally, an advantage in the use of R^2 over a likelihood based approach is that it can be compared over different sample sizes (data must not be thrown out to directly compare different τ values).

We can summarise some positive aspects in the use of this model over the standard approach of equation 1. Our approach is easier because it can account for different lags in the delayed density dependence with a fixed number of parameters. This is an important point for data having a time scale finer than one year. Detecting a two-year delay for bimonthly data using the standard approach implies the estimation of thirteen parameters, an impracticable task because of the curse of dimensionality. In our approach, all model parameters can be related to biological quantities that regulate the individual dynamics, and potentially can be measured empirically. This allows independent estimation from other demographic studies, important to perform a consistency check of the autoregressive estimation. In contrast, in the standard approach, parameters β_i are just statistical parameters for fitting general delayed density-dependent effects in the population growth rate. This difference is important if our interest is modelling rather than just detecting delayed density dependence. Finally, we model our population at the fundamental level of abundance and not to the derived level of the growth-rate.

Results and Discussion

The analysis presented in Fig. 5 shows that the first positive R^2 value is found for $\tau = 3$, which corresponds to 6 months. Temporal delays in population responses can result from the time it takes for many intrinsic (e.g. reproductive event, mortality of young) and extrinsic factors (e.g. predator, competition, parasite infection) to result in changes in population parameters³⁹. These delays are directly related to a number of life-history traits, such as generation time, time of first reproduction, maternal care, reproductive strategy, as well as the species trophic position and the environmental conditions a population faces at a certain moment. In *Didelphis aurita*, a 6-month delay corresponds to the time it takes for the newborn females to reach sexual maturity and start reproducing, also becoming more trappable²⁷. This is the simpler explanation for the positive 6-month delay in our model. The model present two terms, controlled by parameter b and c , both characterised by a 6-month time delay. Together they are the responsible for the regulatory process of the population: low population sizes when individuals are born result in $bx_{t-\tau} > cx_{t-\tau}^2$, a positive contribution to the population 6-months later; larger population sizes when individuals are born quickly results in $bx_{t-\tau} < cx_{t-\tau}^2$, a negative contribution to population size 6-months later. Annual growth rates in this population are most sensitive to changes in the survival of pouch young, the newborns of the season^{40,41}. Therefore, the negative density dependence more likely reflects density dependence in survival rates of pouch young. Adult and aged-adult age classes have the relatively highest contributions to fertility⁴¹, hence more subtle density dependent effects may occur through contributions to fertility by adults and aged adults. However, these would correspond to time delays of 12 months or more as the condition of adults at the start of the breeding season will depend on the conditions of previous seasons, a maternal effect⁴².

The next positive R^2 value is naturally found for a multiple of this value, but not for other τ values. This is the first impressive consistency check between our model outputs and independent measurement of the biological population. Interestingly, the fact that $R^2 < 0$ for $\tau = 1$ rules out the possibility of using the considered autoregressive model without any delay for successfully describing our data. No delay in our time series would have no biological support as well.

The generation of a simulated time series from the stochastic model of equation 2 is straightforward. We fix the numerical values of the parameters a , b , c and σ^2 corresponding to the autoregressive estimation of the best fit model for $\tau = 3$ (see Table 1). Selected the initial conditions X_1, X_2, X_3 from the real data, we obtain a simulated sequence of X_t values. The simplicity of this approach allows the generations of a number of different trajectories produced by our model which turn out to be a powerful strategy for testing our hypothesis. In fact, we can probe if our model well incorporate the stochastic mechanism underlying real data and if it can effectively reproduce the basic patterns of the observed time series.

First, we can reproduce the general behaviour of the empirical time series, as shown in the scatter plot of X_{t+1} versus X_t of Fig. 2. More importantly, starting from the synthetic series, we can replicate the essential trend of the population growth-rate (see Fig. 3), with a clear density-dependent limitation on growth for high population sizes. This finding is very significant. It proves that equation 2 can perfectly account for the density dependent effects present in our empirical data: an approximately linear dependence of the population growth rate with the log population size. This result is remarkable because it is obtained modelling the abundance time series and not directly the growth rate, as in standard approaches of the type of equation 1. In fact, if we use the model of equation 1 we are able to well reproduce the growth rate behaviour, but, in this case, this result is quite obvious, as the

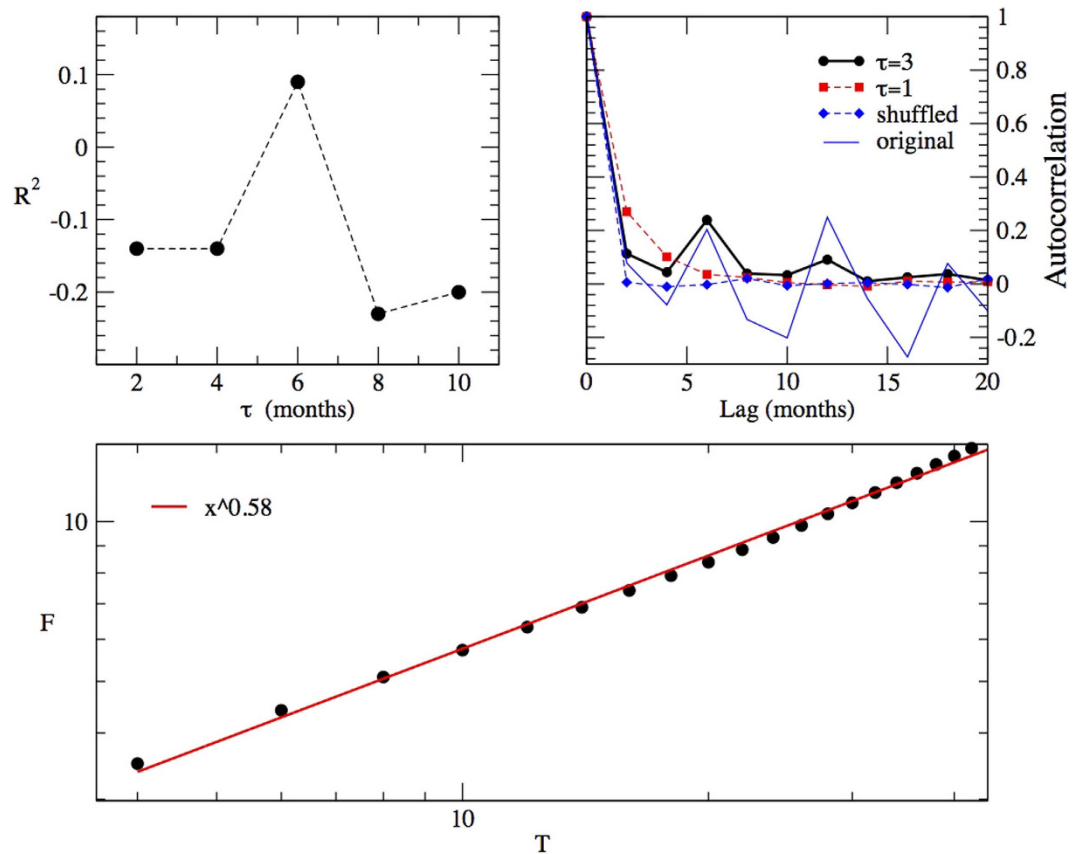


Figure 5. Top, on the left: the R^2 value for different τ . Top, on the right: the autocorrelation function of the synthetic series generated by the best fit model, with added noise, for $\tau = 3$ and $\tau = 1$. Blu points are obtained with a random shuffling of the series obtained for $\tau = 3$. From the comparison, we can appreciate the statistical relevance of the autocorrelation values. Bottom: DFA analysis of the synthetic series generated by the model parametrised as in Table 1 with added noise.

Parameter	Estimate	Standard Error	<i>t</i>	<i>P</i>
a	0.134	0.102	1.314	0.197
b	1.514	0.243	6.230	<0.001
c	-0.029	0.007	-4.143	<0.001

Table 1. Parameter estimates and associated significance levels for the autoregressive model with $\tau = 3$.

autoregression is a direct fitting procedure over the population growth rate. All these results are robust and have been tested for different simulation runs and for long simulations of up to 10000 time steps.

In the following, we examine the correlations behaviour of the simulated time series. For this reason, we generate long simulated series, with at least 1000 events, which permit robust statistical analysis. The resulting simulated series present positive correlation values at lag of 6 months and its multiples, a result comparable with the output of the real data analysis (see Fig. 5). The analysis of the time series generated by the model by means of the DFA method results in an exponent α compatible with the one of the real data (see Fig. 5). This fact suggests that the elaborated model can capture some aspects of the essential time correlations present in real data. Only the oscillating behaviour caused by the anti-correlated values that follows the positive peaks are lost in our model.

One of the most interesting aspect of our autoregressive model is that all the parameters can be directly biologically interpreted and, potentially, estimated empirically. The parameter *a* corresponds to the survival fraction of the population that contributes with the population size two months later. For this reason, its estimated value should be $0 < a < 1$. The parameter *b* is proportional to the fertility, and in order to maintain a positive equilibrium population and compensate the mortality, should be $b > 1 - a^{36,43}$. The parameter *c* controls the reduction in fertility for high populated communities. In principle, also this parameter can be related to basic measurable quantities⁴³. It is the responsible for the density-dependent pattern in the population growth rate and should be negative. We can highlight some plausible factors that could be associated to this parameter. Resource limitation is more likely the main mechanism of density-dependence. However, disease cannot be disregarded because of the relatively high load of parasites in animals in the area. In addition, high population density may have at least

three different effects on future population size through reproduction: (1) prevents active females to reproduce through strong intraspecific competition for food and space, (2) reduces the number of fertilised females by forcing males to disperse due to intraspecific competition, with possible modifications in movements strategies⁴⁴, and (3) forces newborn young to disperse to adjacent areas, with a final reduction in local population size estimates.

These constraints limiting the values of model parameters were always respected in our analyses, for all values of τ . Additional analyses performed using the time series generated by different population size estimates (minimum number known alive, ad hoc estimators for each sampling session) confirm these results. These facts corroborate the robustness of our modelling approach. In particular, our estimated values for $\tau = 3$ satisfy the condition $1 - a < b < 3(1 - a)$ which states that the model equilibrium solution is locally stable³⁶. A final proof of the functionality of our model is the similarity between our a value evaluation compared with an independent empirical measurement: the value estimated by the model corresponds to $a \approx 0.2$, the same found in a demographic study of the same population of opossums²⁷, hardly a coincidence.

The possibility of robustly reproducing general qualitative patterns with a relatively short time series is a relevant and novel contribution presented here⁴⁵. In addition, population size fluctuations of an organism living in an environment as complex as the Atlantic forest produce time series of high variance and noise, adding difficulty to the task. Detecting evidence of density-dependent dynamic behaviour is by far not new, but being able to reproduce directly the dynamics of the abundance time series based on biologically realistic and measurable parameters is. Our model incorporates the basic demographic characteristics operating in a natural population: the temporal delay due to reproduction peculiarities, fecundity and survival rates, and the effect of density-dependence on reproduction.

References

- Berryman, A. A. & Kindlmann, P. *Population systems: a general introduction* (Springer Science & Business Media, New York, 2008).
- Sibly, R. M., Barker, D., Denham, M. C., Hone, J. & Pagel, M. On the regulation of populations of mammals, birds, fish, and insects. *Science* **309**, 607–610 (2005).
- Lande, R., Engen, S. & Saether, B. E. *Stochastic population dynamics in Ecology and Conservation* (Oxford University Press, Oxford, 2003).
- Henderson, P. A. & Magurran, A. E. Direct evidence that density-dependent regulation underpins the temporal stability of abundant species in a diverse animal community. *Proc. R. Soc. B: Biol. Sci.* **281**, 1791 (2014).
- Turchin, P. *Complex population dynamics: a theoretical/empirical synthesis* (Princeton University Press, Princeton, 2003).
- Grenfell, B. T. *et al.* Noise and determinism in synchronized sheep dynamics. *Nature* **394**, 674 (1998).
- Fryxell, J. M., Falls, J. B., Falls, E. A. & Brooks, R. J. Long-term dynamics of small-mammal populations in Ontario. *Ecology* **79**, 213–225 (1998).
- Ferguson, J. M. & Ponciano, J. M. Evidence and implications of higher order scaling in the environmental variation of animal population growth. *Proceedings of the National Academy of Sciences* **112**, 2782–2787 (2015).
- Royama, T. *Analytical Population Dynamics* (Chapman & Hall, London, 1992).
- Lima, M., Ernest, S. K. M., Brown, J. H., Belgrano, A. & Stenseth, N. C. Chihuahuan Desert kangaroo rats: Nonlinear effects of population dynamics, competition, and rainfall. *Ecology* **89**, 2594–2603 (2008).
- Berryman, A. & Lima, M. Deciphering the effects of climate on animal populations: diagnostic analysis provides new interpretation of soay sheep dynamics. *Am. Nat.* **168**, 784–795 (2006).
- Boonstra, R. & Krebs, C. J. Population dynamics of red-backed voles (*Myodes*) in North America. *Oecologia* **168**, 601–620 (2012).
- Ellner, S. & Turchin, P. Chaos in a noisy world: new methods and evidence from time-series analysis. *Am. Nat.* **145**, 343–375 (1995).
- Dennis, B. & Taper, M. L. Density dependence in time series observations of natural populations: estimation and testing. *Ecol. Monog.* **64**, 261–282 (1994).
- Bjornstad, O. N., Falck, W. & Stenseth, N. C. A geographical gradient in small rodent density fluctuations: a statistical modelling approach. *Proc. R. Soc. Lond. B* **262**, 127–133 (1995).
- Turchin, P. & Millstein, J. A. EcoDyn/RSM: response surface modeling of nonlinear ecological dynamics. *Applied Biomathematics* (Setauket, New York, 1993).
- Berryman, A. & Turchin, P. Identifying the density-dependent structure underlying ecological time series. *Oikos* **92**, 265–270 (2001).
- Ahrestani, F. S., Hebblewhite, M. & Post, E. The importance of observation versus process error in analyses of global ungulate populations. *Sci. Rep.* **3**, 3125 (2013).
- Mendel, S. M., Vieira, M. V. & Cerqueira, R. Precipitation, litterfall, and the dynamics of density and biomass in the black-eared opossum, *Didelphis aurita*. *J. Mammal.* **89**, 159–167 (2008).
- White, G. C. & Burnham, K. P. Program MARK: Survival estimation from populations of marked animals. *Bird Study* **46**, Supplement, 120–138 (1999).
- Burnham, K. P. & Anderson, D. R. *Model selection and multimodel inference. A practical information-theoretic approach* (Springer Science Media Inc., New York, United States of America 2002).
- Aanes, R., Sæther, B.-E. & Øritsland, N. A. Fluctuations of an introduced population of Svalbard reindeer: the effects of density dependence and climatic variation. *Ecography* **23**, 437–443 (2000).
- Murúa, R., González, L. A. & Lima, M. Population dynamics of rice rats (a Hantavirus reservoir) in southern Chile: feedback structure and non-linear effects of climatic oscillations. *Oikos* **102**, 137–145 (2003).
- Lima, M., Berryman, A. A. & Stenseth, N. C. Feedback structures of northern small rodent populations. *Oikos* **112**, 555–564 (2006).
- Lima, M., Julliard, R., Stenseth, N. C. & Jaksic, F. M. Demographic dynamics of a neotropical small rodent (*Phyllotis darwini*): feedback structure, predation and climatic factors. *Journal of Animal Ecology* **70**, 761–775 (2001).
- Leirs, H. *et al.* Stochastic seasonality and nonlinear density-dependent factors regulate population size in an African rodent. *Nature* **389**, 176–180 (1997).
- Kajin, M., Cerqueira, R., Vieira, M. V. & Gentile, R. Nine-year demography of the black-eared opossum *Didelphis aurita* (Didelphimorphia: Didelphidae) using life tables. *Revista Brasileira de Zoologia* **25**, 206 (2008).
- Oli, M. K., Holler, N. R. & Wooten, M. C. Viability analysis of endangered Gulf Coast beach mice (*Peromyscus polionotus*) populations. *Biological Conservation* **97**, 107 (2001).
- Gentile, R., Finotti, R., Rademaker, V. & Cerqueira, R. Population dynamics of four marsupials and its relation to resource production in the Atlantic forest in Southeastern Brazil. *Mammalia* **68**, 109–119 (2004).
- Marquet, A. P. *et al.* Scaling and power-laws in ecological systems. *The Journal of Experimental Biology* **208**, 1749 (2005).
- Peng, C. K. *et al.* Mosaic organization of DNA nucleotides. *Phys. Rev. E* **49**, 1685 (1994).
- Morariu, V. V., Buimaga-Iarinca, L., Vamos, C. & Soltuz, C. Detrended Fluctuation Analysis of Autoregressive Processes. *Fluct. Noise Lett.* **7**, L249 (2007).

33. Galhardo, C. E. C., Penna, T. J. P., Argollo de Menezes, M. & Soares, P. P. S. Detrended fluctuation analysis of a systolic blood pressure control loop. *New Journal of Physics* **11**, 103005 (2009).
34. Kantelhardt, J. W. *et al.* Detecting long-range correlations with detrended fluctuation analysis. *Physica A* **295**, 441–454 (2001).
35. Allen, K. R. Analysis of stock-recruitment relations in Antarctic fin whales. *Cons. Int. pour l'Exptor. Mer-Rapp. et Proc.-Verb.*, **164**, 132 (1963).
36. Clark, C. W. A Delayed-Recruitment Model of Population Dynamics, with an Application to Baleen Whale Populations. *Journal of Mathematical Biology* **3**, 381 (1976).
37. Victor, J. D. & Canel, A. A Relation Between the Akaike Criterion and Reliability of Parameter Estimates, with Application to Nonlinear Autoregressive Modelling of Ictal EEG. *Annals of Biomedical Engineering* **20**, 167 (1992).
38. Turchin, P. Nonlinear Time-Series Modeling of Vole Population Fluctuations. *Res. Popul. Ecol.* **38**, 121 (1996).
39. Hudson, P. J., Dobson, A. P. & Newborn, D. Prevention of Population Cycles by Parasite Removal. *Science* **282**, 2256–2258 (1998).
40. Cerqueira, R., Gentile, R., Fernandez, F. A. S. & D' Andrea, P. S. A five-year population study of an assemblage of small mammals in southeastern Brazil. *Mammalia* **57**, 507–517 (1993).
41. Ferreira, M. S. *et al.* Life history of a neotropical marsupial: Evaluating potential contributions of survival and reproduction to population growth rate. *Mammalian Biology* **78**, 406–411 (2013).
42. Beckerman, A., Benton, T. G., Ranta, E., Kaitala, V. & Lundberg, P. Population dynamic consequences of delayed life-history effects. *Trends in Ecology and Evolution* **17**, 263–269 (2002).
43. Murray, J. D. *Mathematical Biology* (Springer-Verlag Berlin Heidelberg 2002).
44. Almeida, P. J. A. L. *et al.* What if it gets crowded? Density-dependent tortuosity in individual movements of a Neotropical mammal. *Austral Ecology* **40**, 758–764 (2015).
45. Rademaker, V. & Cerqueira, R. Variation in the latitudinal reproductive patterns of the genus *Didelphis* (Didelphimorphia: Didelphidae). *Austral Ecol.* **31**, 337–342 (2006).

Acknowledgements

We are grateful to generations of Laboratório de Vertebrados students that make possible such a long term field work. We also thank A. Marcondes, N. Barros, R. Juazeiro and R. S. Honorato for technical and clerical help. This work has been supported by grants to RC from CAPES, CNPq, FAPERJ, PELD/MCT/CNPq, PROBIO II/MCT/MMA/GEF, and PPBio/CNPQ.

Author Contributions

E.B., M.V.V., M.K., M.A.d.M. and R.C. conceived the paper; data were collected by the team of R.C. and M.V.V.; M.K. generated the time series estimates; E.B. and M.A.d.M. analysed the time series; E.B., M.K., M.V.V., R.C. and P.J.A.L.A. interpreted the results; E.B., M.V.V., M.K. and P.J.A.L.A. wrote the manuscript. All authors reviewed the manuscript.

Additional Information

Competing financial interests: The authors declare no competing financial interests.

How to cite this article: Brigatti, E. *et al.* Detecting and modelling delayed density-dependence in abundance time series of a small mammal (*Didelphis aurita*). *Sci. Rep.* **6**, 19553; doi: 10.1038/srep19553 (2016).



This work is licensed under a Creative Commons Attribution 4.0 International License. The images or other third party material in this article are included in the article's Creative Commons license, unless indicated otherwise in the credit line; if the material is not included under the Creative Commons license, users will need to obtain permission from the license holder to reproduce the material. To view a copy of this license, visit <http://creativecommons.org/licenses/by/4.0/>